Background Note on DFAIR

October 26, 2023

Advice on Background Notes for DICE-2022: These background notes are for informational purposes for modelers. They are not intended for publication and are not publication quality. Some of the details are sketched and not derived in detail in this document. They may be cited with the warning, "Background notes are for informational purposes and are not published."

I. Summary

This note describes the calibration of the Finite Amplitude Impulse-Response (FAIR) model for DICE-2022, labeled "DFAIR." Part I is the calibration to climate-carbon models. Part II is harmonization with historical data. The appendix shows details from the calculations.

The DFAIR carbon-cycle model differs from the earth-science literature in using a five year step. Otherwise, it is essentially equivalent to the Millar et al. (2017) implementation and tracks closely the adaptation of Dietz et al. (2021). For the climate module, it uses the calibration of Millar et al. (2017) with a simple two-box climate model. We have tested alternative parameterizations. They perform differently for different tests, and we have found the Millar et al. (2017) specification sufficiently close to adopt that for the DFAIR model.

The key findings are the following:

First, the Millar et al. (2017) specification of FAIR tracks closely both carbon cycle models and the historical data on emissions and concentrations. The DFAIR model tends to underestimate concentrations relative to the Joos et al. (2013) multi-model simulations. Additionally, it tends to underpredict concentrations slightly in both the carbon cycle models and for the historical data.

Second, for large pulses (the 5000 GtC pulse estimate by Joos), all versions of the FAIR model behave poorly in the short run (up to 100 years), but they are reasonably close for the longer run.

Third, looking at the two major simulations (100GtC and 5000 GtC), the FAIR model is successful in capturing the saturation in carbon absorption that results in higher atmospheric retention in the large compared

to the small pulse. This is a notable advance over the linear carbon models used in earlier vintages of the DICE and most other IAMs.

The calibration of initial conditions for FAIR is difficult because it is path-dependent. We have created a "1765 model" of the DFAIR GAMS version that runs from 1765 to 2020. Using this, we made a successful splice with the 2020 initial conditions based on the 1765 model.

Fourth, the climate model does a reasonable job of capturing the dynamics and does not need structural revisions from earlier versions of DICE. However, the DFAIR model uses the equation structure of the Millar version, which makes interpretation easier.

Finally, it should be emphasized that the carbon cycle models underlying the multi-model calibrations in Joos et al. (2003) are quite divergent. For example, the 5% - 95% confidence interval for the 100-year time integrated impulse response function for concentrations is 30 – 75 years.

The major open issue is whether the FAIR model's parameters should be adjusted to reflect its shortcomings. This is a larger project and awaits further research.

II. Calibration to climate/carbon cycle models.

The DFAIR model uses the structure derived by Millar et al. (2017), with five year steps. It takes all parameters from the original Millar estimates. The only difference is that the DFAIR model has an equilibrium temperature sensitivity (ETS) of 3.0 °C per CO2 doubling.

We then examined three estimates for the carbon cycle and one test for the climate model. Two of the calibrations were to Joos et al. (2013) multimodel study. Note that according to AR6: "Although there has been greater understanding since AR5 of the carbon cycle responses to CO2 emissions 27 (Chapter 5, Sections 5.4 and 5.5), there has been no new quantification of the response of the carbon-cycle to an instantaneous pulse of CO2 emission since Joos et al. (2013)." Note as well that the models underlying Joos appear to have a neutral biosphere, so that feature misses any interaction with increased carbon uptake in that sector. However, Millar appears to capture land uptake, but the impact of this uptake on parameters is unclear.

I. Carbon cycle

The testing of alternative approaches to the carbon cycle used three pulse tests (100 GtC from pre-industrial conditions, 5000 GtC from pre-industrial conditions, and 100 GtC from 2010 levels) and one run that tested the accuracy of matching historical data on CO2 emissions and concentrations.

i. Pulse tests for 100 GtC from pre-industrial conditions

We began with two pulses from pre-industrial concentrations and compared with Joos et al. (2013). We used the Millar specification of the FAIR model, DFAIR, with five year steps for the comparisons. These tests were not precise for Joos because of the divergence among models. One pulse was 100GtC from pre-industrial conditions (PIC) and the second was 5000GtC from PIC. We also tested alternative parameters to see which would be a better fit (labeled "Best").

Figure 1 shows the key results for the atmospheric retention. The Millar et al. (2017) parameters have lower atmospheric retention than Joos et al. (2013) or the other specifications, particularly at short horizons. The "best" parameters match very closely.

Figure 2 shows the temperature response to the same pulse. The temperature results are reversed, with Millar et al. (2017) having lower temperature than Joos et al. (2013) even though the atmospheric concentrations are lower. This result comes from the difference in the climate models in Joos et al. (2013) and the FAIR 2-equation climate model. There are two versions of Millar. One uses an ETS of 3.0 °C, while the other uses a lower value of 2.75 °C. Both are low relative to the Joos models.

While the temperature models relative to Joos are divergent, the DFAIR version of the climate model matches the IPCC AR6 climate estimates exactly, so this suggests that the problem is the Joos climate models rather than the DFAIR climate model.

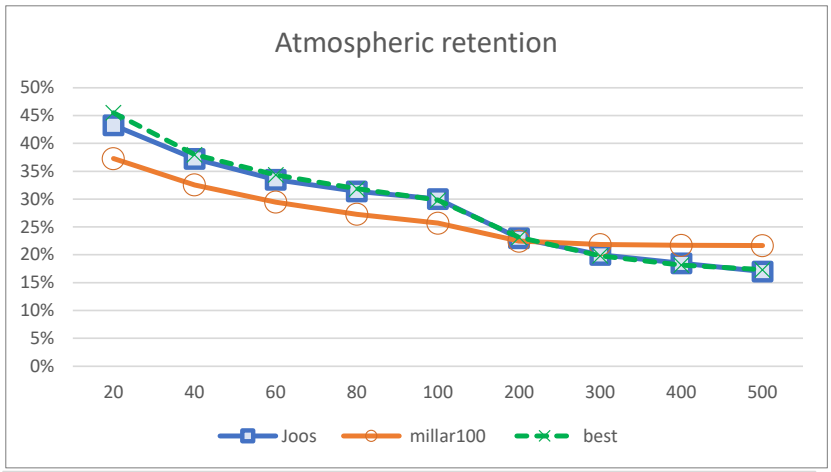

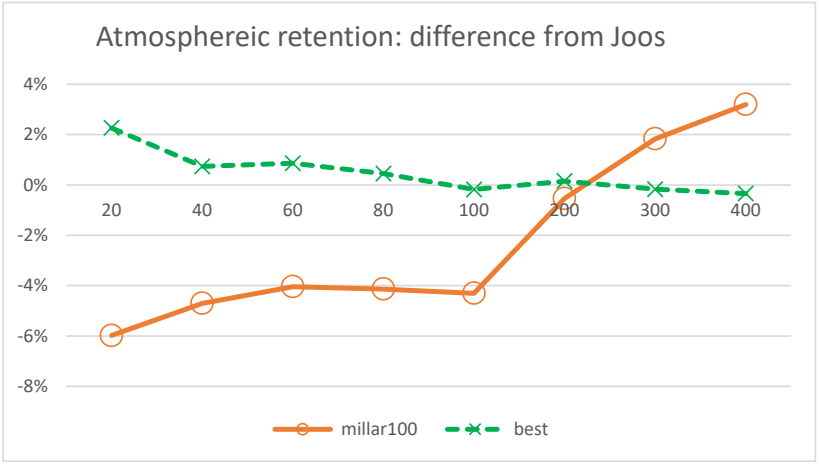

Figure **DFAIR-**1. Atmospheric retention, alternative specifications, pulse of 100 GtC from PIC (years).

(Source: Tests=FAIR-sept0122.xls)

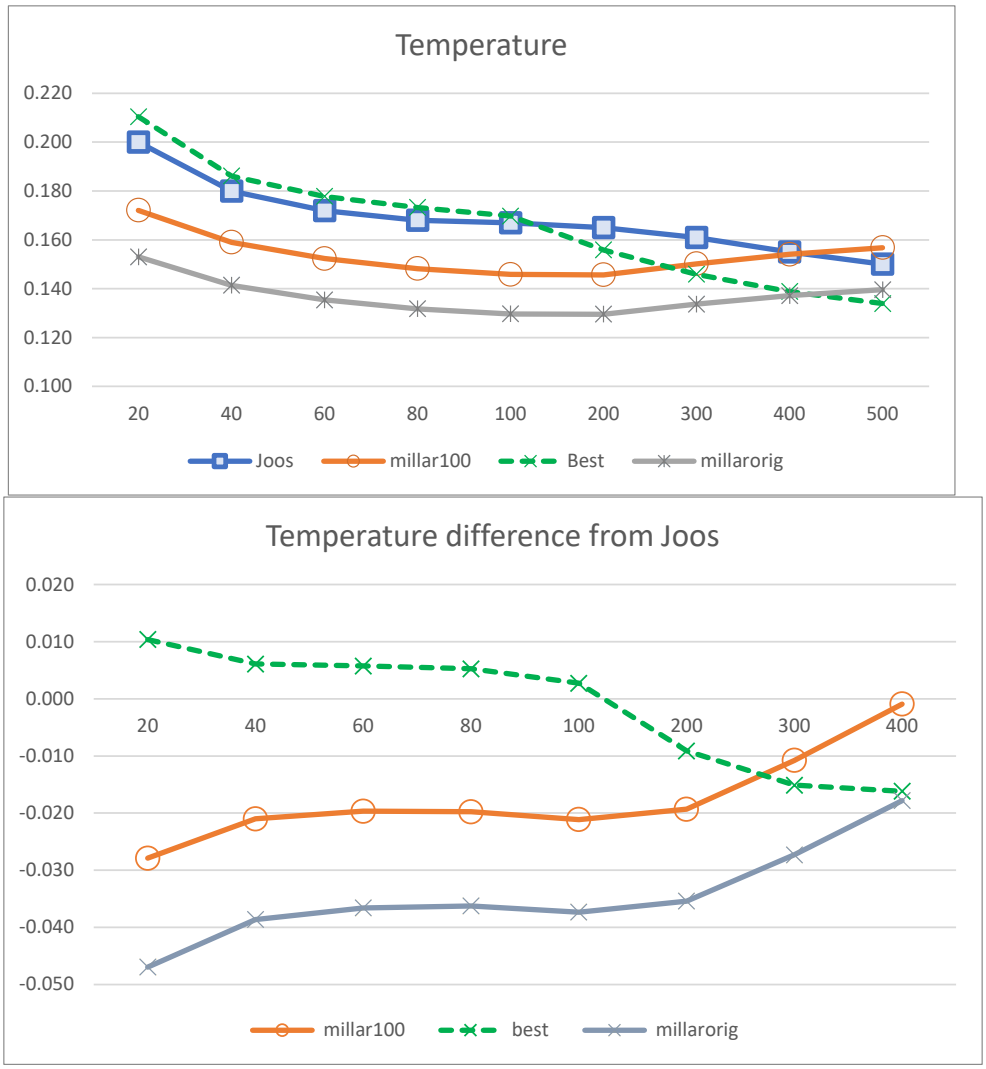

Figure **DFAIR-**2. Results of 100GtC pulse on temperature at different time horizons (years).

(Source: Tests=FAIR-sept0122.xls)

ii. Pulse test for 5000 GtC from pre-industrial conditions

We performed identical runs for a very large pulse, 5000 GtC. For reference, cumulative emissions to date are approximately 2000 GtC by 2100 in the base run and 1400 GtC in the optimal run. The point of this test is to see how well FAIR reproduces the saturation of larger models.

Figure 3 shows the results for the atmospheric retention. FAIR does reasonably well from about 60 years forward, although it tends to have lower convexity than the full earth-system models in Joos et al. (2013). This non-convexity seems to hold for all model parameters, and FAIR therefore tends to understate concentrations for the first half-century (as was the case for the 100 GtC pulse as well). Figure 4 shows the results for temperature (using the higher ETS). The simple climate model fails to capture the shape of the full models after 100 years. The reason for the difference is unclear and is probably not due to the error in the atmospheric retention.

However, the most important result is that the model definitely captures the saturation with high pulses. Note, comparing figures 1 and 3, that the atmospheric retention rises from 30% with the small shock to 70% with the large shock at 100 years. Linear carbon cycle models, such as those used in earlier DICE models and other studies, would have identical percentages.

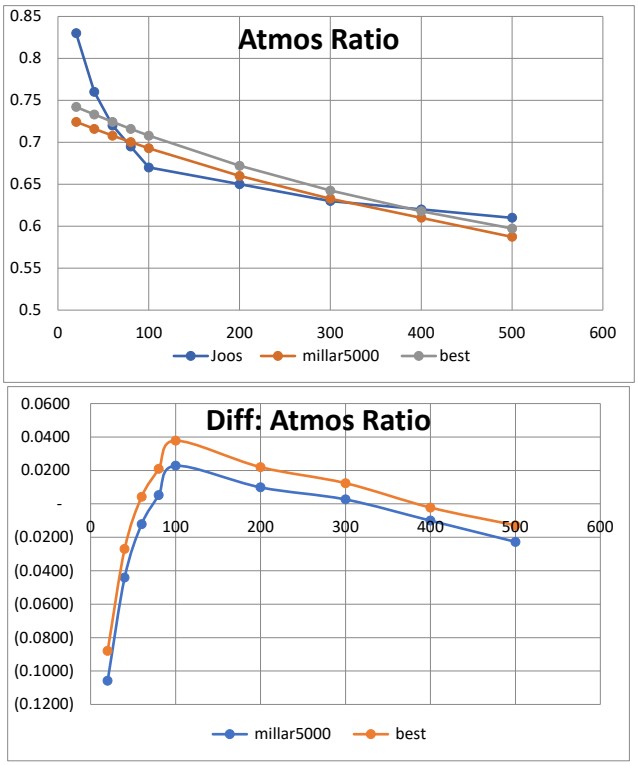

Figure **DFAIR-**3. Atmospheric retention of CO2 for 5000 GtC pulse

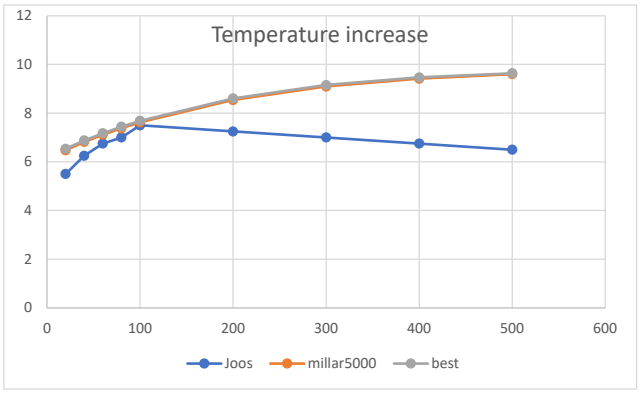

Figure **DFAIR-**4. Temperature increase (°C) for 5000 GtC pulse

iii. <u>100 GtC from 2010 levels (389 ppm)</u>

The third pulse test considered 100 GtC again but against background concentrations which are otherwise held constant at 2010 levels assumed to be 389 ppm (829.42 GtC), in line with both Joos et al. (2013) and the key results reported also in Dietz et al. (2021). For this test, we modify the finel

DFAIR model from DICE-2023 based on the experimental conditions of Joos et al. and Dietz et al. In particular, we (i) follow Dietz et al. in distributing the corresponding initial excess atmospheric CO2 concentrations over pre-industrial levels (829.42 – 588 = 241.4 GtC) into the four carbon reservoirs according to 52.9% in box 1; 34.3% in box 2; 11.1% in box 3; 1.6% in box 4; (ii) assuming 0.85 ◦ C as initial atmospheric warming relative to pre-industrial and lower ocean warming of 0.22°C. (by setting initial temperature in Box 1 to 0.22°C and in Box 2 to 0.63°C so that TATM0 = 0.85°C); (iii) assuming 531 GtC as initial cumulative emissions as in Dietz et al.; (iv) adopting the baseline emissions scenario from Dietz et al. to keep concentrations absent the pulse approximately constant (specifically by adding up annual emissions underlying Dietz et al. into 5-year totals and taking the average per period as value for ECO2); (v) assuming zero non-CO2 forcings as in Dietz et al., noting that experimentation with assuming initial year non-CO2 forcings to be constant at initial year levels had only a minimal impact (+0.001-0.002◦C) on the estimated temperature response. One notable difference from Dietz et al. is that we do not assume an equilibrium climate sensitivity of 3.1°C (which they impose across models) but retain the DFAIR benchmark value of 3.0°C in line with IPCC AR6.

The results of the 100 GtC pulse test in this environment are shown in Appendix Figure D-1. The results indicate that the DFAIR model addresses the critique of Dietz et al. (2021) and others that prior vintages of DICE exhibited excessive warming inertia in response to emissions impulses compared to recent climate model estimates as shown in Joos et al. (2013). It does, however, again also indicate that DFAIR initially underpredicts warming levels slightlyl in the near term, and overpredicts slightly in the longer run.

iv. *Comparison with history*

The final comparison is to use FAIR to project concentrations from 1765 to 2020. For this purpose, we used actual CO2 emissions as best coult be reconstructed from IPCC, CDIAC, and EDGAR. We then constrained both CO2 emissions and non-CO2 forcings using the data from AR6. The emissions were from Table 5.1, while the non-CO2 forcings were from Table AIII.3, and were interpolated. We then ran the model from pre-industrial concentrations starting in 1765.

This specification overpredicted temperature signficantly in 2020 (1.515 °C v. 1.25 °C from IPCC). Additionally, it overpredicted ppm but only slightly (422.5 v 417.1 ppm).

We then created a "1765 run" to match CO2 concentrations. The 1765 run adjusted both emissions and non-CO2 forcings to better track history. This run slightly underpredicted 2020 ppm (414.7 v 417.1 ppm actual) but matched tempeature (1.248). We then used the 2020 values here for calibration of the DICE-2020 model. The following shows the assumptions and results for the different scenarios and history.

		1900	1950	2000	2020
CO2 emissions (GtCO2)					
	Uncalibrated	6.2	11.2	30.0	40.5
	Calibrated	5.4	9.9	30.0	40.5
	IPCC total	3.5	7.6	27.4	36.6
	DICE	2.0	6.2	25.7	37.7
Non-CO2 forcings (W/m2)					
	Uncalibrated	0.00	0.06	0.46	0.68
	Calibrated	-0.10	-0.04	0.06	0.28
	History	-0.01	-0.06	0.46	0.68
Concentrations (ppm)					
	Uncalibrated	291.9	311.6	373.1	422.5
	Calibrated	289.8	306.8	366.7	414.7
	History	295.7	311.3	370.0	414.0
Temperature (from 1765)					
	Uncalibrated	0.19	0.39	1.05	1.52
	Calibrated	0.11	0.29	0.80	1.25
	History	0.13	0.30	0.87	1.25

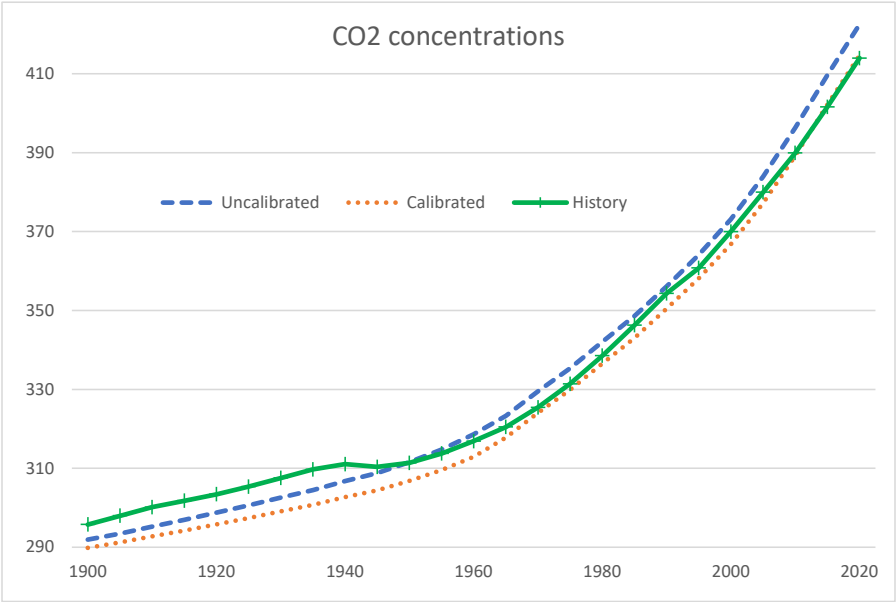

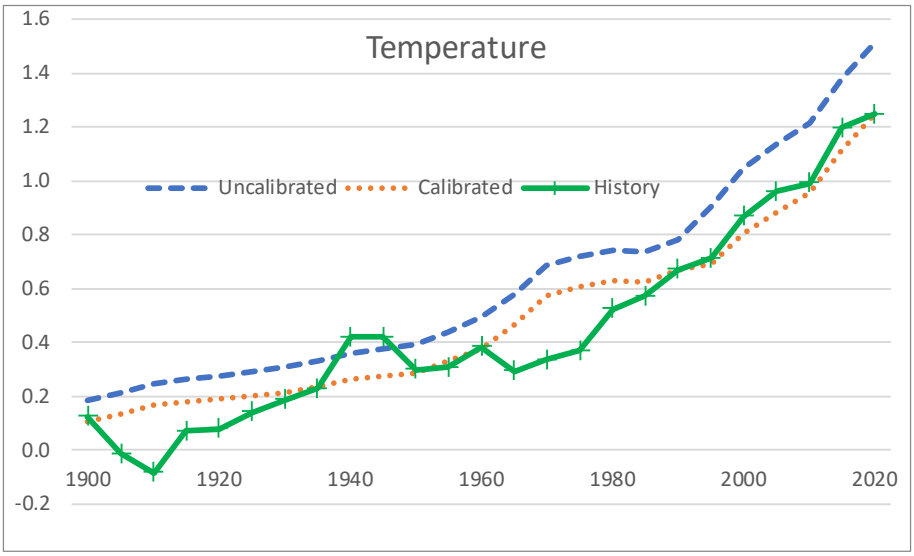

Table DFAIR-1 and Figure DFAIR-5. Comparison of FAIR model variants with history and two scenarios for emissions and forcings

Source: DICE2022A-base-3-11-1765-Runs.xlsx.

II. Climate Module

The FAIR climate module is analytically similar to that in DICE-2016. It is a two-equation model with five parameters (see appendix for the equations). We have adopted four of the five, which represent the dynamics, but have changed the temperature sensitivity from 2.75 °C to 3.0 °C.

We then ran a standard test for the dynamics of the model using stylized CO2 concentrations. This involved 1% concentration growth from pre-industrial concentrations to doubling and then constant concentrations after that. Table 2 shows the transient and equilibrium temperature sensitivity (transient is average around 70 after the start of the growth). The DFAIR does fine here.

	DFAIR	IPCC-AR6
TSC	1.80	1.80
ESC	3.00	3.00

TSC = transitory sensitivity coefficient = temperature increase at 60-80 years
ESC = equilibrium sensitivity coefficient
Units are degrees C from pre-industrial conditions

Table DFAIR-2. Behavior of DFAIR climate module compared to Sixth IPCC Assessment report

[Source: ESC-table-092522u122822.xls]

III. Calibration of history with projections.

The final step is to calculate the initial conditions. (These are listed at the end of this section.) These are the initial stocks in the four carbon reservoirs, cumulative carbon emissions, and the initial temperatures in the two boxes.

To estimate these, we used the "1765 model." This starts in equilibrium in 1765, with all initial stocks in equilibrium. It then puts historical CO2

emissions into the DFAIR model starting in 1765. The simulation uses the calibrated version discussed above.

We then calibrated the DICE model (starting in 2020) with the 1765 model and compared the outputs over the splice period from 2020 to 2035. [update using Millar (adj)]. Table 3 compares the outputs of 1765 model and 2020+ model and shows the splice is essentially perfect.

Period	1	2	3	1
Year	2020	2025	2030	2035
Total CO2 Emissions, GTCO	0.08%	0.48%	1.69%	2.42%
Atmospheric concentration	0.00%	0.02%	0.10%	0.19%
Atmospheric temperaturer	0.00%	0.03%	0.12%	0.26%
Total forcings w/m2	7.72%	0.05%	0.17%	0.34%
Forcings, exogenous w/m2				
CO2 forcings w/m2	0.00%	0.06%	0.20%	0.38%
Total CO2 Emissions, GTCO	0.08%	0.48%	1.69%	2.42%
Permanent C box	0.00%	0.04%	0.15%	0.29%
Slow C box	0.00%	0.06%	0.21%	0.41%
Medium C box	0.00%	0.15%	0.57%	1.06%
Fast C box	0.00%	0.42%	1.49%	2.34%
Temp Box 1	0.00%	0.01%	0.03%	0.06%
Temp Box 2	0.00%	0.03%	0.13%	0.28%
Alpha	0.00%	-0.02%	-0.03%	0.06%
IFR	0.00%	0.00%	-0.01%	0.01%
cacc	0.00%	-0.05%	-0.14%	-0.14%
ccatot	0.00%	0.01%	0.04%	0.15%

Table DFAIR-3. Quality of splice between 1765 model and DICE model.

Percentage difference between the values of 1765 model and DICE-2022 for overlap of splice.

[Source: compare-1765-dice2022-u122822.xls]

The following are the initial conditions for the calibrated version (note that the high resolution figures are from the output of the 1765 model). One important note is that the temperature change is from 1765 and therefore does not always match either the standard calculations from preindustrial or those in damage studies.

```
** INITIAL CONDITIONS TO BE CALIBRATED TO HISTORY
** CALIBRATION
    mat0   Initial concentration in atmosphere in 2020 (GtC)     /886.5128014/

    res00  Initial concentration in Reservoir 0 in 2020 (GtC)      /150.093 /
    res10  Initial concentration in Reservoir 1 in 2020 (GtC)      /102.698 /
    res20  Initial concentration in Reservoir 2 in 2020 (GtC)      /39.534  /
    res30  Initial concentration in Reservoir 3 in 2020 (GtC)      / 6.1865 /

    mateq      Equilibrium concentration atmosphere  (GtC)          /588   /
    tbox10    Initial temperature box 1 change in 2020 (C from 1765)  /0.1477  /
    tbox20    Initial temperature box 2 change in 2020 (C from 1765)  /1.099454/
    tatm0     Initial atmospheric temperature change in 2020         /1.24715 /
```

Appendix DFAIR-1. Parameters of different models.

The basic parameters from Millar et al. (2017) are reproduced in Table A-1.

Table 1. Default parameter values for the simple impulse-response climate–carbon-cycle models used in this paper.

Parameter	Value – AR5-IR	Value – PI-IR	Value – FAIR	Guiding analogues
a_0	0.2173	0.1545	0.2173	Geological re-absorption
a_1	0.2240	0.1924	0.2240	Deep ocean invasion/equilibration
a_2	0.2824	0.2424	0.2824	Biospheric uptake/ocean thermocline invasion
a_3	0.2763	0.4108	0.2763	Rapid biospheric uptake/ocean mixed-layer invasion
τ_0 (year)	1×10^6	1×10^6	1×10^6	Geological re-absorption
τ_1 (year)	394.4	276.7	394.4	Deep ocean invasion/equilibration
τ_2 (year)	36.54	30.75	36.54	Biospheric uptake/ocean thermocline invasion
τ_3 (year)	4.304	4.459	4.304	Rapid biospheric uptake/ocean mixed-layer invasion
q_1 ($KW^{-1}\,m^2$)	0.33	0.33	0.33	Thermal equilibration of deep ocean
q_2 ($KW^{-1}\,m^2$)	0.41	0.41	0.41	Thermal adjustment of upper ocean
d_1 (year)	239.0	239.0	239.0	Thermal equilibration of deep ocean
d_2 (year)	4.1	4.1	4.1	Thermal adjustment of upper ocean
r_0 (year)	–	–	32.40	Preindustrial $iIRF_{100}$
r_C (year GtC^{-1})	–	–	0.019	Increase in $iIRF_{100}$ with cumulative carbon uptake
r_T (year K^{-1})	–	–	4.165	Increase in $iIRF_{100}$ with warming

Table DFAIR-A-1. Parameters in Millar version of FAIR model.

(Source: Millar et al. (2017) , Table 1)

Appendix DFAIR-2. Parameters of Millar Model and Alternatives

Parameters	Millar (orig)	Dietz	DFAIR
emshare0	0.2173	0.2173	0.2173
emshare1	0.2240	0.2240	0.2240
emshare2	0.2824	0.2824	0.2824
emshare3	0.2763	0.2763	0.2763
tau0	1,000,000	1,000,000	1,000,000
tau1	394.4000	394.4000	394.4000
tau2	36.5300	36.5300	36.5300
tau3	4.3040	4.3040	4.3040
teq1	0.3300	0.3300	0.3240
teq2	0.4100	0.4100	0.4400
d1	239.0000	239.0000	236.0000
d2	4.1000	4.1000	4.0700
IRF0	32.4000	34.4000	32.4000
irC	0.0190	0.0190	0.0190
irT	4.1650	4.1650	4.1650
fco22x	3.7400	4.2000	3.9300
mat0	588.0000	588.0000	588.0000

Variable	Units	Definition
emshare0	Fraction	Geological re-absorption
emshare1	Fraction	Deep ocean invasion/equilibration
emshare2	Fraction	Biospheric uptake/ocean thermocline invasion
emshare3	Fraction	Rapid biospheric uptake/ocean mixed-layer invasion
tau0	Year	Geological re-absorption
tau1	Year	Deep ocean invasion/equilibration
tau2	Year	Biospheric uptake/ocean thermocline invasion
tau3	Year	Rapid biospheric uptake/ocean mixed-layer invasion
teq1	$KW^{-1}m2$	Thermal equilibration of deep ocean
teq2	KW-1m2	Thermal adjustment of upper ocean
d1	Year	Thermal equilibration of deep ocean
d2	Year	Thermal adjustment of upper ocean
IRF0	Year	Preindustrial iIRF100
irC	$YearGtC^{-1}$	Increase in iIRF100 with cumulative carbon uptake
irT	$YearK^{-1}$	Increase in iIRF100 with warming
fco22x	$KW^{-1}m2$	Forcings for CO2 doubling
mat0	GtC	Initial carbon stock

Appendix DFAIR-3.. Literature on Carbon Cycle

The following show the results from the Joos et al. (2013) study that are used in the calibrations discussed above.

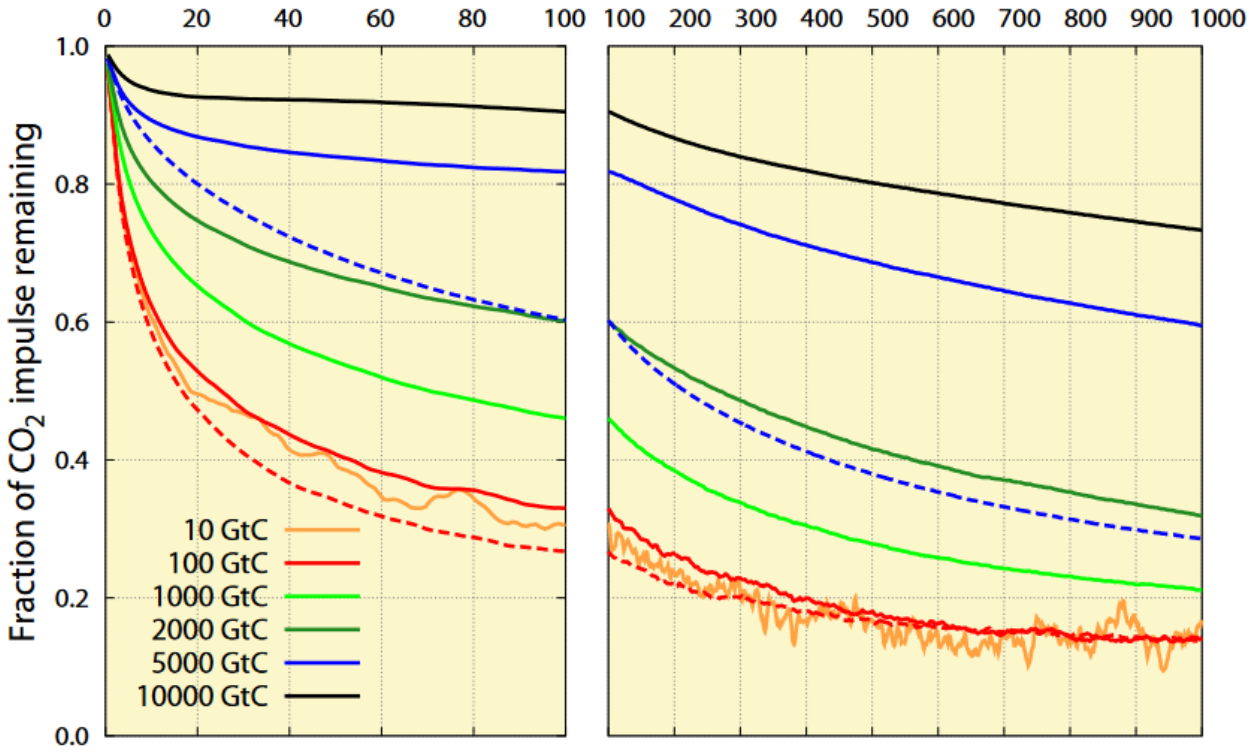

[From Joos et al. (2013): "Fig. 7. Influence of pulse size and climate-carbon cycle feedback on the response in atmospheric CO2 and the time-integrated IRFCO2 as simulated with the Bern3D-LPJ model (standard setup). Pulse emissions, ranging from 10 to 10 000 GtC in the individual simulations, are added to the atmosphere under preindustrial conditions. Dashed lines represent simulations where climate was kept constant in the model."]

A. Results for atmospheric retention of pulses in multimodel:

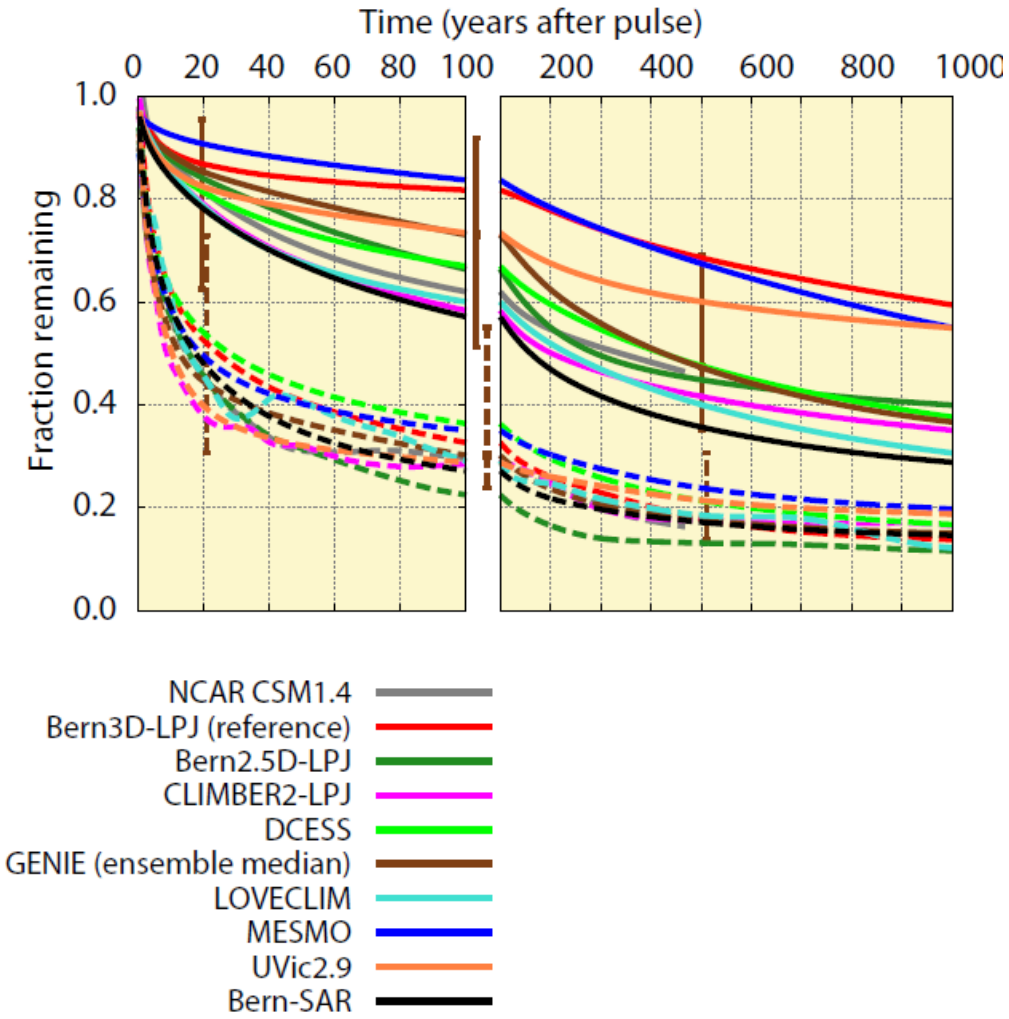

[From Joos et al. (2013): " Fig. 6. Response of the carbon cycle-climate system to a pulse emission of 5000 GtC (solid, PI5000) and 100 GtC (dashed, PI100) added to the atmosphere under preindustrial conditions. The responses in surface air temperature, ocean heat content, steric sea level rise, and in carbon fluxes for PI5000 are scaled by a factor of 50 for a better comparison with the 100 GtC pulse."]

B. Results for temperature to pulses

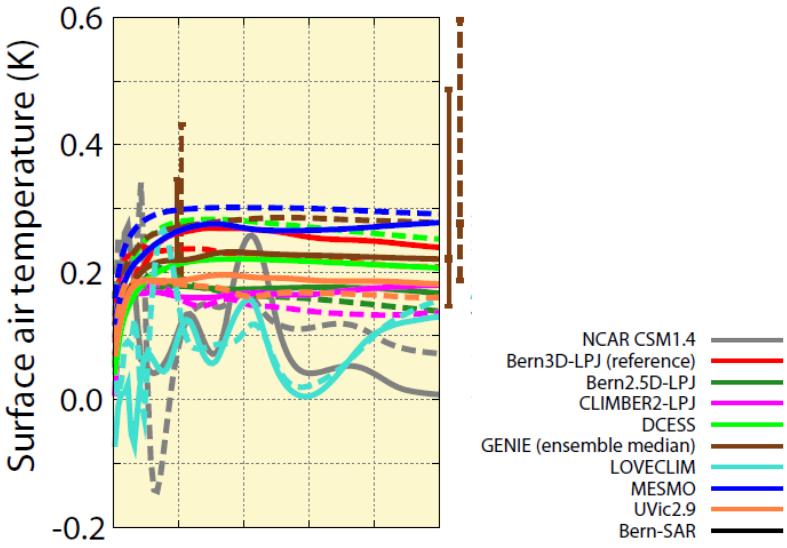

"From Joos et al. (2013): Fig. 4. Influence of the background conditions on the climate-carbon cycle response to a pulse emission of 100 GtC into the atmosphere. Solid lines are for current conditions (CO2, ref = 389 ppm, PD100) and dashed lines for preindustrial conditions (CO2, ref = 280 ppm, PI100)."

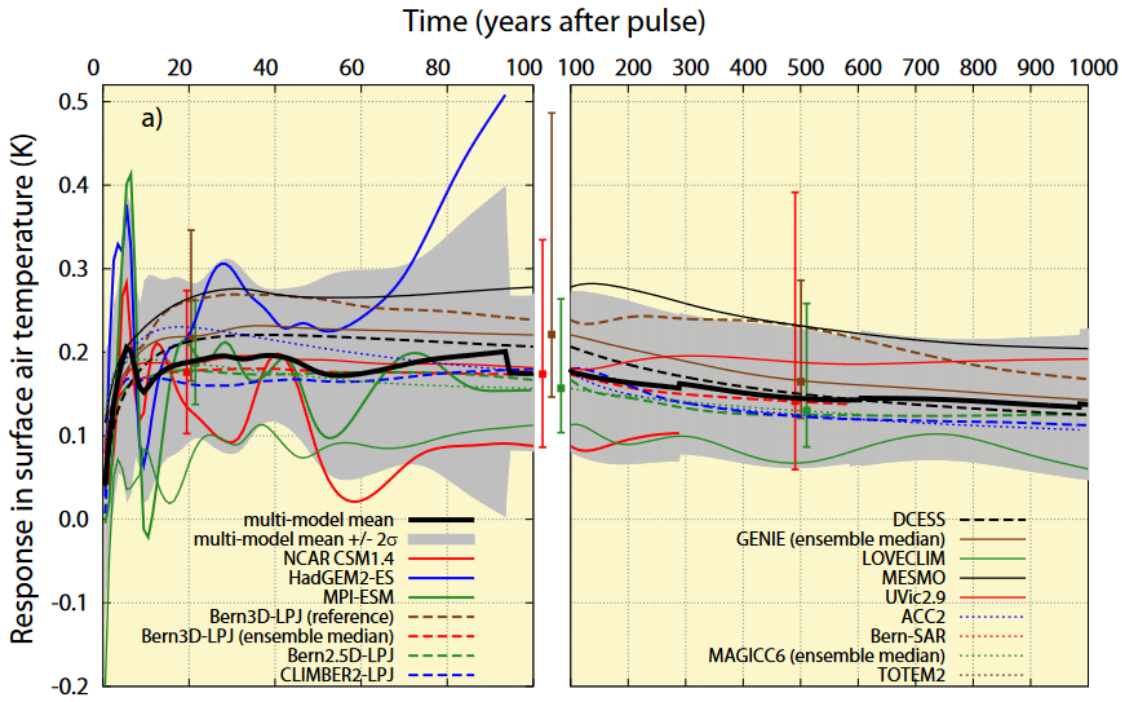

[From Joos et al. (2013): "Fig. 2. As Fig. 1 but for the perturbation in global mean surface air temperature (a), in ocean heat content (b), and in steric sea level rise (c). Results are for a CO2 emission pulse of 100 GtC added to a current CO2 concentration of 389 ppm (PD100).We note that the signal-to-noise ratio is small for the models that feature a dynamic atmosphere (HadGEM2-ES, MPI-ESM, NCAR-CSM1.4, and LOVECLIM) and the plotted evolutions for these models represent both the forced response and a contribution from the models' internal (unforced) climate variability. Small abrupt changes in the multi-model mean and confidence range arise from a change in the number of model simulations; different groups run their model over different periods, pending on CPU availability."]

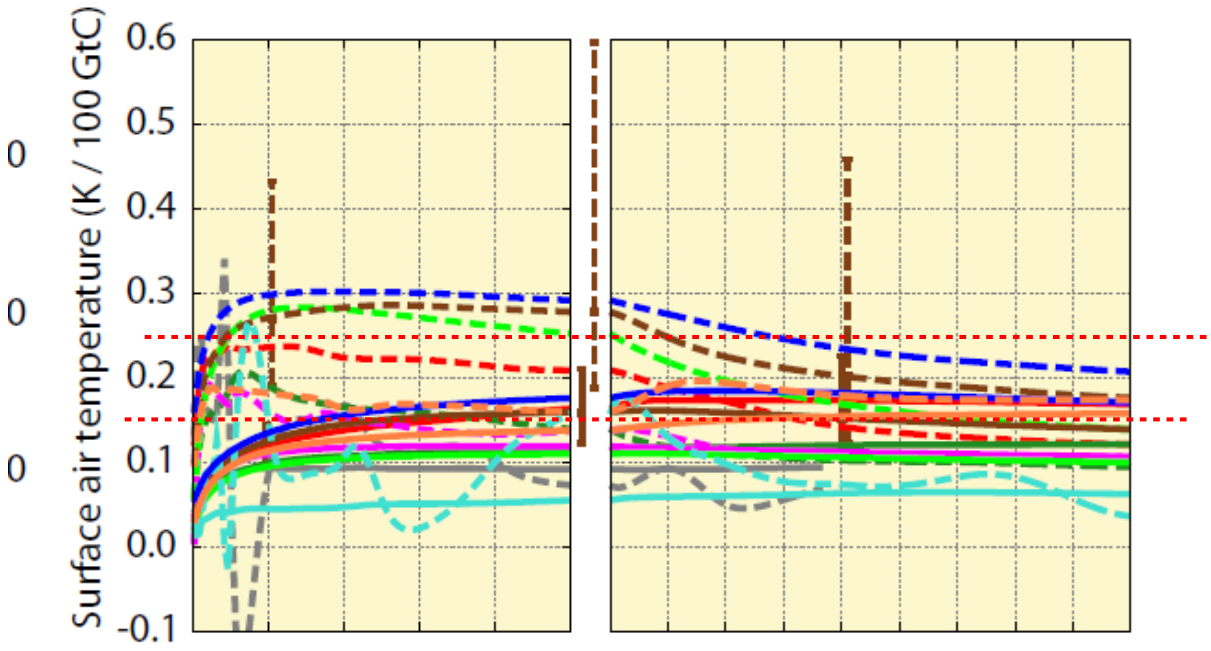

[From Joos et al. (2013): "Fig. 6. Response of the carbon cycle-climate system to a pulse emission of 5000 GtC (solid, PI5000) and 100 GtC (dashed, PI100) added to the atmosphere under preindustrial conditions. The responses in surface air temperature, ocean heat content, steric sea level rise, and in carbon fluxes for PI5000 are scaled by a factor of 50 for a better comparison with the 100 GtC pulse."]

NOTE that Millar et al. (2017) finds roughly the same results in his comparison.

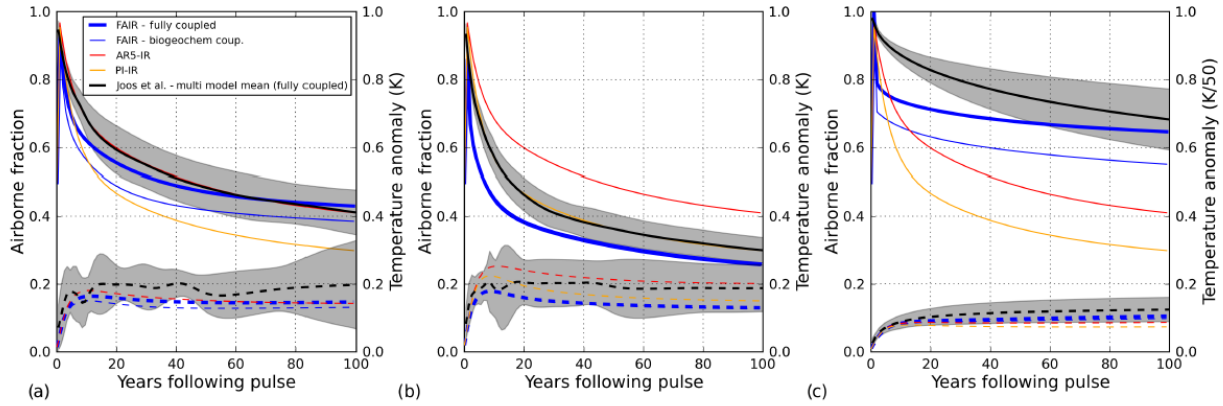

Figure 3. Response to pulse emission experiments of Joos et al. (2013). **(a)** shows the response to a 100 GtC imposed on present-day (389 ppm) background conditions (PD100 experiment), **(b)** the response to a 100 GtC pulse in preindustrial conditions (PI100 experiment) and **(c)** the response to a 5000 GtC pulse in preindustrial conditions (PI5000 experiment) with the warming normalised by the increase in pulse size between **(b)** and **(c)**. Airborne fraction (left-hand axis) is represented by solid lines in all panels and warming (right-hand axis) by dashed lines. FAIR is shown as thick blue lines, AR5-IR as red, and PI-IR as orange. The black lines in all panels shows the Joos et al. (2013) multi-model mean for airborne fraction (solid) and warming (dashed), with the grey shading indicating 1 standard deviation uncertainty across the ensemble. Thin blue lines denote the biogeochemically coupled version of FAIR.

Following is blowup of (b), 100GtC from preindustrial.

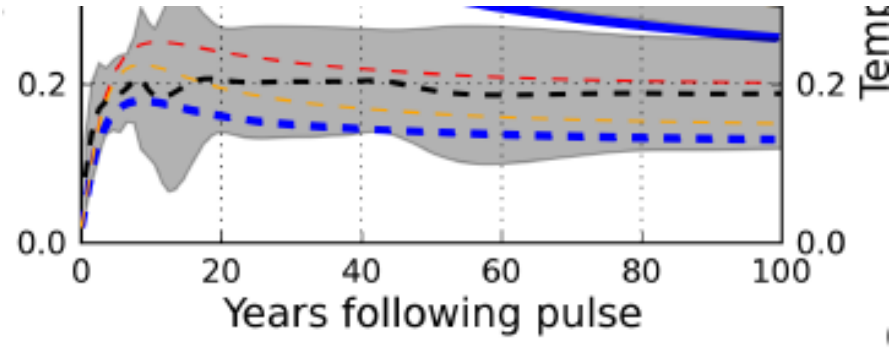

Although there is little discussion of the basic carbon cycle in IPCC AR6, there is discussion of the asymmetry. Figure 5.35 from IPCC AR6 is consistent with the Joos et al. (2013) findings. Median model is 30% retention for a 100GtC pulse from PI conditions.

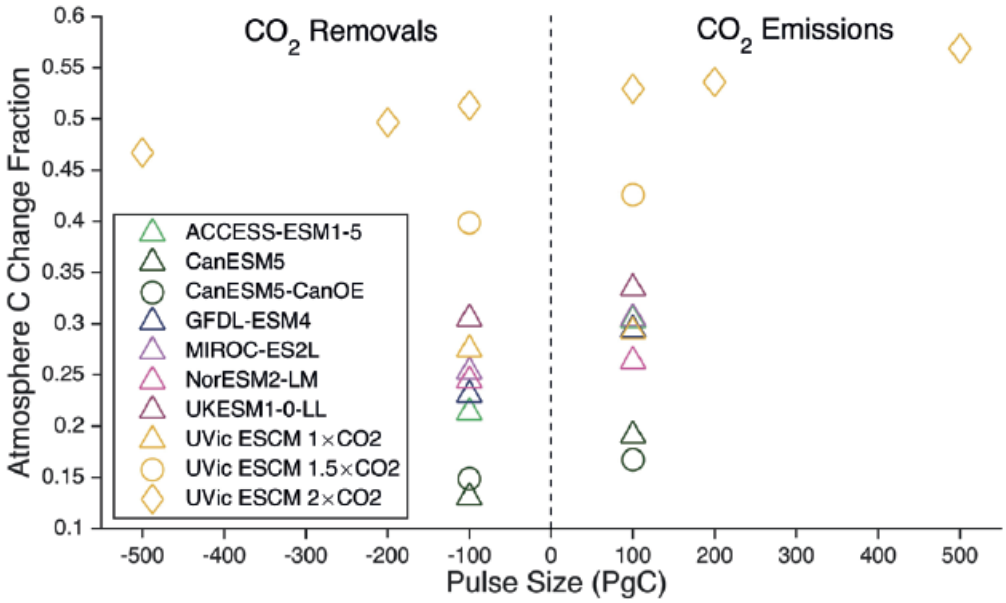

"Figure 5.35 | Asymmetry in the atmospheric carbon dioxide (CO2) response to CO2 emissions and removals. Shown are the fractions of total CO2 emissions remaining in the atmosphere (right-hand side) and CO2 removals remaining out of the atmosphere (left-hand side) 80–100 after a pulse emission/removal. Triangles and green circles denote results for seven Earth system models (ESMs) and the UVic ESCM model of intermediate complexity forced with ±100 PgC pulses applied from a pre-industrial state (1 × CO2) (Carbon Dioxide Removal Model Intercomparison Project (CDRMIP) experiment CDR-pi-pulse; Keller et al., 2018b). Yellow circles and diamonds indicate UVic ESCM results for CO2 emissions/removals applied at 1.5 times (1.5 × CO2) and 2 times (2 × CO2) the pre-industrial CO2 concentration, respectively. Pulses applied from a 2 × CO2 state span the magnitude ±100 PgC to ±500 PgC. UVic ESCM data is from Zickfeld et al. (2021). Further details on data sources and processing are available in the chapter data table (Table 5.SM.6)."

Median model is 30% retention for a 100GtC pulse from PI conditions.

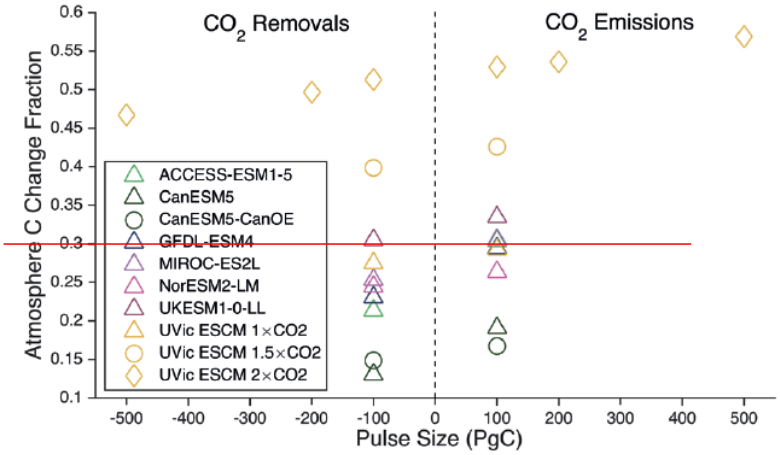

Same as Joos et al. (2013) below:

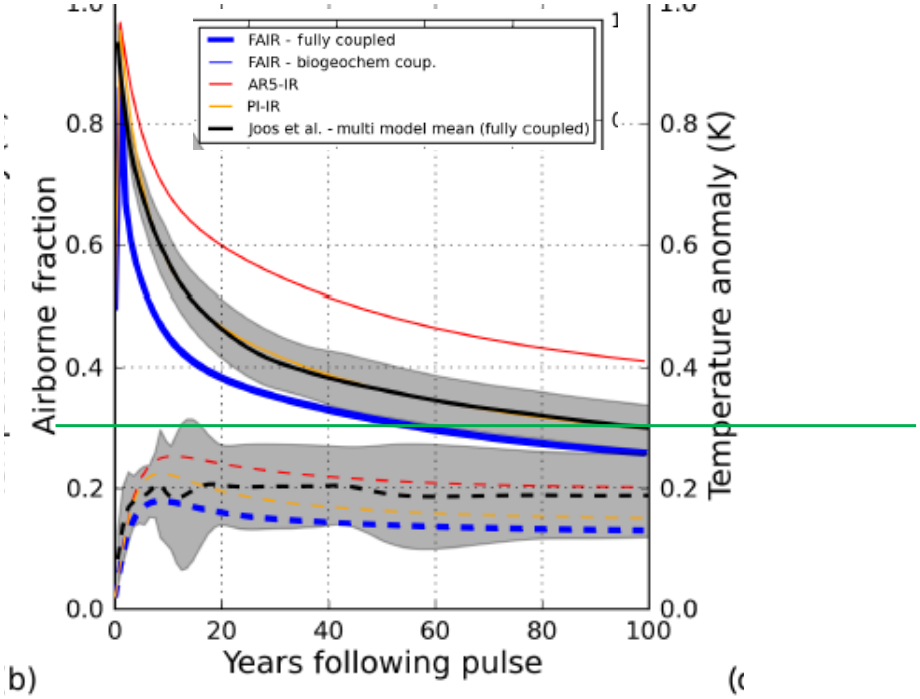

NOTE from AR6: "Although there has been greater understanding since AR5 of the carbon cycle responses to CO2 emissions 27 (Chapter 5, Sections 5.4 and 5.5), there has been no new quantification of the response of the carbon-cycle 28 to an instantaneous pulse of CO2 emission since Joos et al. (2013)."

So, best is to start with calibrating to the 100 year, 100GtC pulse. Here are parameters for best (v1), Millar et al. (2017) , and others. The adjustments necessary are both (1) decrease the permanent share by about .05; and (2) increase the IFR0 by about 7 years. The latter was used by Dietz et al, and the former is necessary to get the asymptote correct.

Parameters		millar100	v1	v2	v3	v4
emshare0 =		0.2173	0.1650	0.1650	0.2173	0.1650
emshare1 =		0.2240	0.2740	0.3040	0.2240	0.2240
emshare2 =		0.2824	0.3324	0.3824	0.2824	0.3824
emshare3 =		0.2763	0.2286	0.1486	0.2763	0.2286
tau0 =		1.00E+06	1.00E+06	1.00E+06	1.00E+06	1.00E+06
tau1 =		394.4000	394.4000	394.4000	394.4000	394.4000
tau2 =		36.5300	36.5300	36.5300	36.5300	36.5300
tau3 =		4.3040	4.3040	4.3040	4.3040	4.3040
teq1 =		0.3300	0.3300	0.3300	0.3300	0.3300
teq2 =		0.4100	0.4100	0.4100	0.4100	0.4100
d1 =		239.0000	239.0000	239.0000	239.0000	239.0000
d2 =		4.1000	4.1000	4.1000	4.1000	4.1000
IRF0 =		32.4000	39.0000	39.0000	39.0000	39.0000
irC =		0.0190	0.0190	0.0190	0.0190	0.0190
irT =		4.1650	4.1650	4.1650	4.1650	4.1650
fco22x =		4.2000	4.2000	4.2000	4.2000	4.2000

Appendix DFAIR-4

The equations of the DFAIR model as of February 2023 are the following. (FAIR-beta-4-3-1.gms)

```
** Equals old FAIR with recalibrated parameters for revised F2xco2 and Millar model.
** Deletes nonnegative reservoirs. See explanation below

sets    tfirst(t), tlast(t);

PARAMETERS
      yr0    Calendar year that corresponds to model year zero        /2020/
     emshare0 Carbon emissions share into Reservoir 0   /0.2173/
     emshare1 Carbon emissions share into Reservoir 1    /0.224/
     emshare2 Carbon emissions share into Reservoir 2    /0.2824/
     emshare3 Carbon emissions share into Reservoir 3    /0.2763/
     tau0    Decay time constant for R0  (year)                    /1000000/
     tau1    Decay time constant for R1  (year)                    /394.4/
     tau2    Decay time constant for R2  (year)      /36.53/
     tau3    Decay time constant for R3  (year) /4.304/

     teq1    Thermal equilibration parameter for box 1 (m^2 per KW)        /0.324/
     teq2    Thermal equilibration parameter for box 2 (m^2 per KW)       /0.44/
     d1     Thermal response timescale for deep ocean (year)            /236/
     d2     Thermal response timescale for upper ocean (year)           /4.07/

     irf0    Pre-industrial IRF100 (year)                          /32.4/
     irC     Increase in IRF100 with cumulative carbon uptake (years per GtC)    /0.019/
     irT     Increase in IRF100 with warming (years per degree K)            /4.165/
     fco22x   Forcings of equilibrium CO2 doubling (Wm-2)                   /3.93/

** INITIAL CONDITIONS TO BE CALIBRATED TO HISTORY
** CALIBRATION
     mat0   Initial concentration in atmosphere in 2020 (GtC)      /886.5128014/
     res00  Initial concentration in Reservoir 0 in 2020 (GtC)     /150.093 /
     res10  Initial concentration in Reservior 1 in 2020 (GtC)     /102.698 /
     res20  Initial concentration in Reservoir 2 in 2020 (GtC)     /39.534  /
     res30  Initial concentration in Reservoir 3 in 2020 (GtC)     / 6.1865 /
     mateq     Equilibrium concentration atmosphere  (GtC)         /588   /
     tbox10    Initial temperature box 1 change in 2020 (C from 1765)  /0.1477  /
     tbox20    Initial temperature box 2 change in 2020 (C from 1765)  /1.099454/
     tatm0     Initial atmospheric temperature change in 2020         /1.24715 /
   ;
VARIABLES
*Note: Stock variables correspond to levels at the END of the period
      FORC(t)       Increase in radiative forcing (watts per m2 from 1765)
      TATM(t)       Increase temperature of atmosphere (degrees C from 1765)
      TBOX1(t)      Increase temperature of box 1 (degrees C from 1765)
      TBOX2(t)      Increase temperature of box 2 (degrees C from 1765)
      RES0(t)       Carbon concentration in Reservoir 0 (GtC from 1765)
      RES1(t)       Carbon concentration in Reservoir 1 (GtC from 1765)
      RES2(t)       Carbon concentration in Reservoir 2 (GtC from 1765)
      RES3(t)       Carbon concentration in Reservoir 3 (GtC from 1765)
      MAT(t)        Carbon concentration increase in atmosphere (GtC from 1765)
      CACC(t)       Accumulated carbon in ocean and other sinks (GtC)
      IRFt(t)       IRF100 at time t
      alpha(t)      Carbon decay time scaling factor
      SumAlpha      Placeholder variable for objective function;
```

```
**** IMPORTANT PROGRAMMING NOTE. Earlier implementations has reservoirs as non-negative.
**** However, these are not physical but mathematical solutions.
**** So, they need to be unconstrained so that can have negative emissions.
NONNEGATIVE VARIABLES   TATM, MAT,  IRFt, alpha
EQUATIONS
      FORCE(t)       Radiative forcing equation
      RES0LOM(t)     Reservoir 0 law of motion
      RES1LOM(t)     Reservoir 1 law of motion
      RES2LOM(t)     Reservoir 2 law of motion
      RES3LOM(t)     Reservoir 3 law of motion
      MMAT(t)        Atmospheric concentration equation
      Cacceq(t)      Accumulated carbon in sinks equation
      TATMEQ(t)      Temperature-climate equation for atmosphere
      TBOX1EQ(t)     Temperature box 1 law of motion
      TBOX2EQ(t)     Temperature box 2 law of motion
      IRFeqLHS(t)    Left-hand side of IRF100 equation
      IRFeqRHS(t)    Right-hand side of IRF100 equation
;
** Equations of the model
   res0lom(t+1)..   RES0(t+1) =E=  (emshare0*tau0*alpha(t+1)*(Eco2(t+1)/3.667))*(1-exp(-
tstep/(tau0*alpha(t+1))))+Res0(t)*exp(-tstep/(tau0*alpha(t+1)));
   res1lom(t+1)..   RES1(t+1) =E=  (emshare1*tau1*alpha(t+1)*(Eco2(t+1)/3.667))*(1-exp(-
tstep/(tau1*alpha(t+1))))+Res1(t)*exp(-tstep/(tau1*alpha(t+1)));
   res2lom(t+1)..   RES2(t+1) =E=  (emshare2*tau2*alpha(t+1)*(Eco2(t+1)/3.667))*(1-exp(-
tstep/(tau2*alpha(t+1))))+Res2(t)*exp(-tstep/(tau2*alpha(t+1)));
   res3lom(t+1)..   RES3(t+1) =E=  (emshare3*tau3*alpha(t+1)*(Eco2(t+1)/3.667))*(1-exp(-
tstep/(tau3*alpha(t+1))))+Res3(t)*exp(-tstep/(tau3*alpha(t+1)));
   mmat(t+1)..      MAT(t+1)  =E=   mateq+Res0(t+1)+Res1(t+1)+Res2(t+1)+Res3(t+1);
   cacceq(t)..      Cacc(t)   =E=  (CCATOT(t)-(MAT(t)-mateq));
   force(t)..       FORC(t)   =E=  fco22x*((log((MAT(t)/mateq))/log(2))) + F_Misc(t)+F_GHGabate(t);

   tbox1eq(t+1)..   Tbox1(t+1) =E=  Tbox1(t)*exp(-tstep/d1)+teq1*Forc(t+1)*(1-exp(-tstep/d1));
   tbox2eq(t+1)..   Tbox2(t+1) =E=  Tbox2(t)*exp(-tstep/d2)+teq2*Forc(t+1)*(1-exp(-tstep/d2));
   tatmeq(t+1)..    TATM(t+1)  =E=   Tbox1(t+1)+Tbox2(t+1);
   irfeqlhs(t)..    IRFt(t)   =E=  ((alpha(t)*emshare0*tau0*(1-exp(-100/(alpha(t)*tau0))))+(alpha(t)*emshare1*tau1*(1-exp(-
100/(alpha(t)*tau1))))+(alpha(t)*emshare2*tau2*(1-exp(-100/(alpha(t)*tau2))))+(alpha(t)*emshare3*tau3*(1-exp(-
100/(alpha(t)*tau3)))));
   irfeqrhs(t)..    IRFt(t)   =E=  irf0+irC*Cacc(t)+irT*TATM(t);
**  Upper and lower bounds for stability
MAT.LO(t)       = 10;
TATM.UP(t)      = 20;
TATM.lo(t)      = .5;
alpha.up(t) = 100;
alpha.lo(t) = 0.1;
* Initial conditions
MAT.FX(tfirst)    = mat0;
TATM.FX(tfirst)   = tatm0;
Res0.fx(tfirst) = Res00;
Res1.fx(tfirst) = Res10;
Res2.fx(tfirst) = Res20;
Res3.fx(tfirst) = Res30;
Tbox1.fx(tfirst) = Tbox10;
Tbox2.fx(tfirst) = Tbox20;
** Solution options
option iterlim = 99900;
option reslim = 99999;
option solprint = on;
option limrow = 0;
option limcol = 0;
```